CHARACTERIZATION OF CFRP LAMINATES UNDER TENSION-TENSION FATIGUE USING 3D DIGITAL IMAGE CORRELATION

Nora Schorer [1], Markus G. R. Sause[1]

[1]Institute of Materials Resource Management, University of Augsburg, D-86135 Augsburg, Germany
Email: nora.schorer@mrm.uni-augsburg.de

Abstract

Tension-tension fatigue tests were conducted on cross-ply laminates of carbon fibre reinforced polymers (CFRP). The tests were performed in the low-cycle fatigue range to determine the initial occurrence of damage.
Due to the presence of 90° layers transverse to the tensile direction, primarily inter-fibre cracks occur, which span the entire specimen width and lead to local concentration of deformation. Using 3D high resolution digital image correlation (3D DIC), inter-fibre cracks were detected as such local strain concentrations on the narrow side of the flat specimens. This allows access to information about the initiation of inter-fibre cracks, their local distribution and the amount of strain concentration. In addition, acoustic emission (AE) measurements were carried out. It has been shown that results of both methods can be correlated. Based on this finding, the individual advantages of both methods for crack detection and characterization can be used for further investigation in fatigue experiments.

1. Introduction

The occurrence of damage in composites is very complex due to the anisotropy and inhomogeneity of the material. There is a range of failure types on microscopic and macroscopic scale [1]. In principle, the occurrence and extent of damage depends on the load direction and the load level. Any failure in a material under external load affects the local stress state and thus the local strain state in the material and leads to a change of local mechanical response, which can be explained by the concept of stress concentration. If failure within a certain area exceeds a critical level, the material fails globally [2, 3]. Especially in the cyclic range, a critical accumulation of damage under repetitive load is an important aspect, since it limits the service life [4, 5]. The amount of damage causing fatigue failure is still difficult to assess, which is challenging for composite lifetime prediction. Models for damage accumulation exist, but a global damage accumulation approach can be complicated since global material properties do not necessarily characterize occurrence of local damage that can already lead to final failure [6, 7].
Therefore, this work follows the approach of describing and characterizing the local failure behaviour in composite materials. Secondary measurement methods such as digital image correlation (DIC) and acoustic emission (AE) were used. Both methods have already been used successfully to assess the damage in fatigue testing independently of each other [8, 9]. Using digital image correlation it was possible to carry out measurements to assess the time of initiation, the distribution and the amount of failure of individual events. Furthermore, by combination of both methods it was possible to cross-validate the position of single cracks.

2. Experimental

2.1. Specimen preparation

The specimens were manufactured from Sigrafil CE 1250-230-39 carbon/epoxy prepreg, which was cured at 130 °C and 8 bar according to the recommendations of the material supplier. In order to create inter-fibre cracks during fatigue loading, the layup configuration is chosen as $[0/90_2]_{sym}$. Specimens have

a nominal thickness of 1.32 mm, a width of 30 mm and a clamping length of 150 mm. Tabs of a length of 55 mm made from glass fibre reinforced polymer are adhesively bonded to the specimens (cf. Figure 1b).

2.2.   Measurement setup

Cyclic measurements were carried out on a servo-hydraulic machine (8801MT Instron) with a 100kN load cell. The measurements were load-controlled with a frequency of 2 Hz and a load ratio of R = 0.1. Each test has a duration of 10000 cycles, which includes a fading start of 300 cycles before the maximum load was reached. The maximum load of specimen 1-3 is 16 kN, of specimen 4 is 15 kN, of specimen 5 is14 kN and of specimen 6 is13 kN.

As first secondary measurement method, a high resolution 3D digital image correlation system (ARAMIS 12M GOM) was used with two cameras using a resolution of 4096 x 3072 pixels and a camera lens with a focal length of 50 mm and a lens speed of f/2.8. For all tests one image was taken every 10th cycle, 50N below the maximum load peak. The deformation was measured on the narrow side of the specimen in the area between the sensors for acoustic emission with a measurement field of 100 mm x 1.32 mm (see Figure 1).

As additional secondary measurement method, we used acoustic emission analysis with two WD sensors (see Figure 1). A 2/4/6 preamplifier with a gain of 40 dB$_{AE}$ and an analogue bandpass filter from 20 kHz to 1MHz is used. For the acoustic emission acquisition the threshold of 35 dB$_{AE}$, the sampling rate of 10MSP/s and trigger settings of 10 (PDT), 80 (HDT) and 300 (HLT) were used. The WD sensors were applied to the specimen at a distance of 100 mm.

(a)   (b)
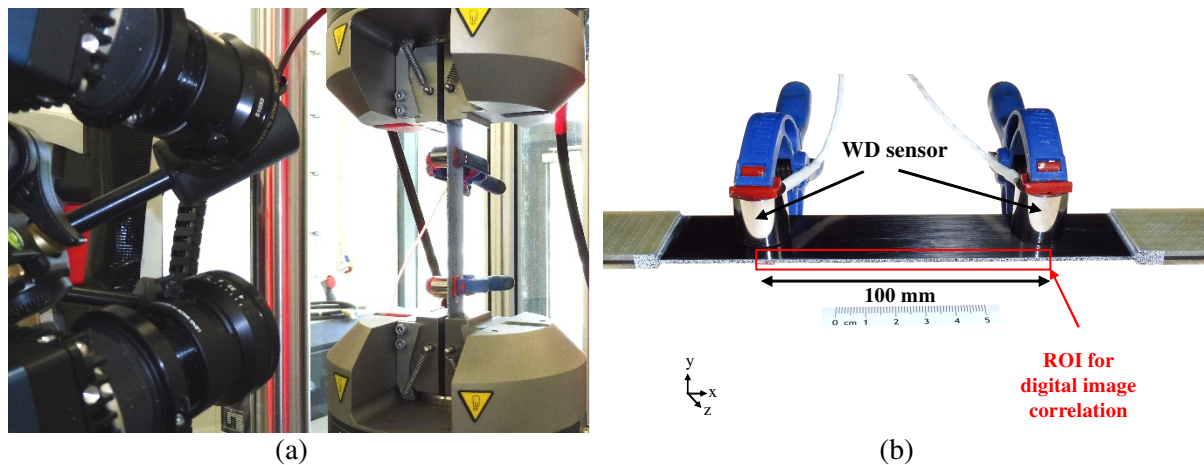
Figure 1. Measurement setup with stereo camera system for digital image correlation (a) and position of the WD sensors on the sample for acoustic emission (b).

2.3. Date reduction

The axial strain for all samples was evaluated as part of the digital image correlation measurements. The subset size was 15 px × 15 px with a distance of the subset centres of 9 px. The resulting spatial resolution was 27.1 μm/px.
In addition to the global axial strain field, the local axial strain of each individual crack was determined. According to equation (1), the local strain at the crack position is calculated from the mean of several subsets m (typically $m = 15$).

$$\overline{\varepsilon}_{local} = \frac{1}{m} \sum_{i=1}^{m} \varepsilon_i \tag{1}$$

Nora Schorer, Markus G. R. Sause

The strain difference results from the local strain average of 5 images after and 5 images before crack formation (see formula 2).

$$\Delta\varepsilon = \frac{1}{5}\sum_{j=1}^{5} \overline{\varepsilon}_{\text{local after, j}} - \frac{1}{5}\sum_{k=1}^{5} \overline{\varepsilon}_{\text{local before, k}} \tag{2}$$

For the evaluation of the local strain concentration of a crack, $\Delta\varepsilon$ can be normalized by the maximum stress level to obtain comparable numeric values for all measurements (cf. [10]), whereby the maximum cycle load was used for the stress calculation.

For the acoustic emission analysis, linear source localization was performed for all measurements using the measured sound velocity of the laminate and time-of-flight measurements. Only events with an absolute energy larger than or equal to 0.2×10^{-4} J were used for the correlation with the macroscopic inter-fibre cracks, since acoustic emission signals with much lower energy result from microscopic damage, which does not result in measurable strain concentration.

3. Results

In the following, the results of the digital image correlation with regard to the potential for damage detection and characterization are presented and are subsequently compared with the acoustic emission data.

3.1. Digital image correlation

It has been shown that with the use of digital image correlation, strain signatures of inter-fibre cracks can be clearly detected. Inter-fibre cracks occur in all specimens during the test (10000 cycles in total). Figure 2 shows the axial strain field of five different cycle numbers of specimen 1 on the narrow side of the specimen. While during 1000 cycles 10 cracks with an average crack spacing of 9.74+/-15.53 mm occur, after 10000 cycles there are 54 cracks with average crack spacing of 1.85+/-0.69 mm. The increasing number of cracks reduces the average crack spacing. In addition, the standard deviation for the sample with 54 cracks is small, since approximately constant and homogeneous crack spacing over the length of the sample is expected when reaching crack density saturation (cf. Figure 5 at 10000 cycles). According to Li et al. [11], in which various GFRP laminates were examined, cracks saturate up to a third of total fatigue life. An evaluation of the measured crack saturation is provided in Figure 3. For the specimens loaded to a maximum load of 16 kN the average crack density is 0.50 cracks/mm after 10000 cycles. For specimen 4 (loaded to 15 kN) the crack density is 0.33 cracks/mm, for specimen 5 (loaded to 14 kN) and for specimen 6 (loaded to 13 kN) the crack density is 0.09 cracks/mm. Due to the lower peak load, the total number of cracks is reduced and they also start to appear later in the test. While 50 % of the cracks in specimens 1 and 2 have already occurred at 3000 cycles, only occasional cracks occur in specimens 5 and 6 at this number of cycles.

Nora Schorer, Markus G. R. Sause
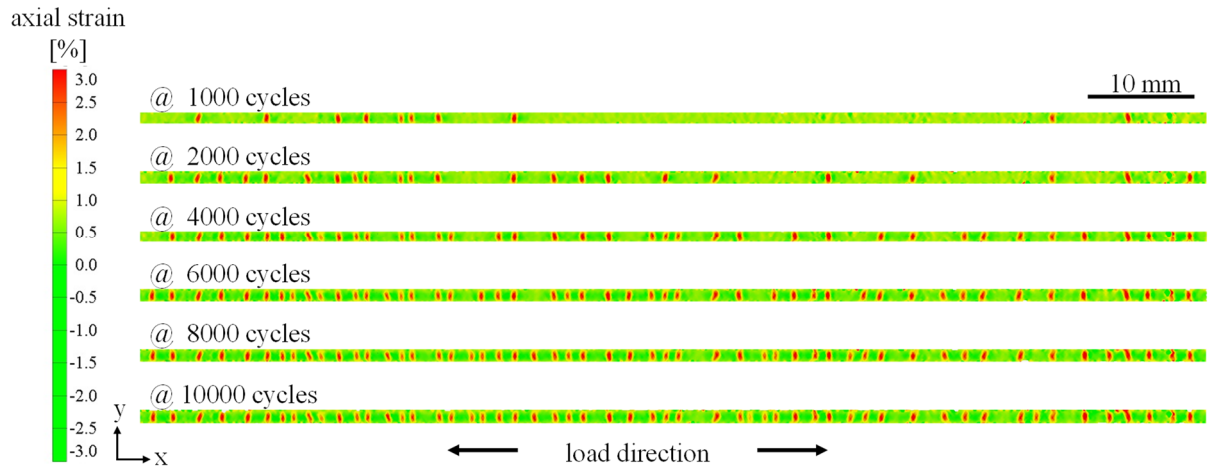
Figure 2. Axial strain field of specimen 1 with strain concentrations at the crack positions at different cycle numbers.
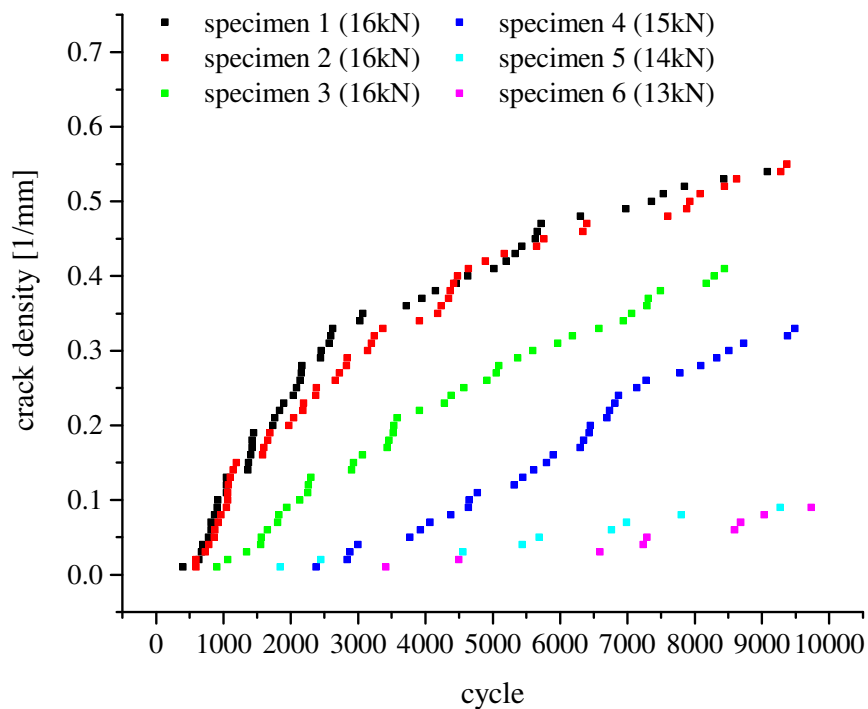
Figure 3. Crack density as function of cycles for each specimen tested.

The formation of inter-fibre cracks leads to an increase in local stress, which results in a local increase of strain. Due to the finite width of the strain concentration field of a single crack, strain fields of neighbouring cracks are superimposed. As evaluation example, the axial strain curves of the individual cracks 1-3 in specimen 1 are shown in Figure 4a. Figure 4b shows xy-sections of the axial strain fields recorded at different cycles. The strain concentration of cracks 1-3 are shown before and after their occurrence including their next neighbours to evaluate their influence. The image of 1728 cycles in Figure 4b shows the strain field before appearance of cracks 1-3. The strain field in the area between the cracks is almost homogeneous, whereas a local reduction of strain is observed close to the two crack positions. At the occurrence of crack 2 at 1760 cycles, a significant strain concentration happens directly at the crack position (red curve in Figure 4a). With appearance of crack 3 at 5032 cycles, the local strain between both cracks decreases due to the mutual influence of the strain fields. This also has an effect on the strain concentration at crack 2, which decreases abruptly directly at 5032 cycles. Crack 1 has formed at 6304 cycles, which again causes a sudden drop in the strain concentration of crack 2. However, this

is not as strong as for crack 3, since it is location is farther away from crack 2 when compared to crack 3.
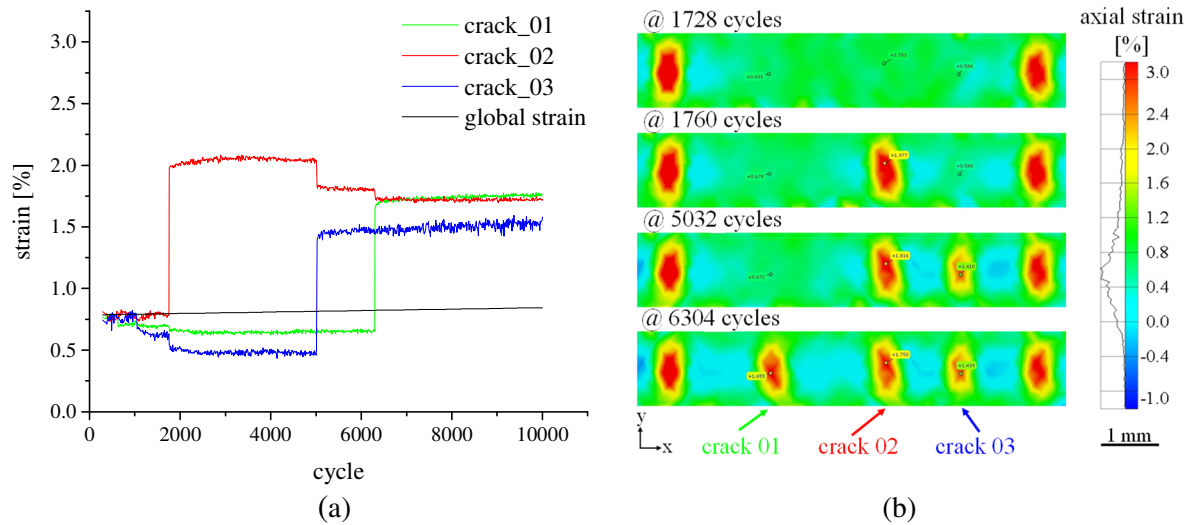
Figure 4. Local axial strain as function of cycles for three adjacent cracks (a) and axial strain field of three adjacent cracks at specific cycles (b).

According to subsection 2.3, a measure of the strain concentration of a single crack refers to the difference of the local strain directly before and after the occurrence of the crack, since the local superposition of the neighbouring cracks must also be considered. In order to compare all specimens, the strain concentration is normalized to the maximum stress used in the fatigue test cycles. The normalized strain concentration of the cracks is independent of the number of cycles the specimen has undergone. Nevertheless, a scattering of the strain concentration of cracks within a specimen and between the specimens is observed, originating from the variations of the crack geometries and from the measurement inaccuracy of the strain field.
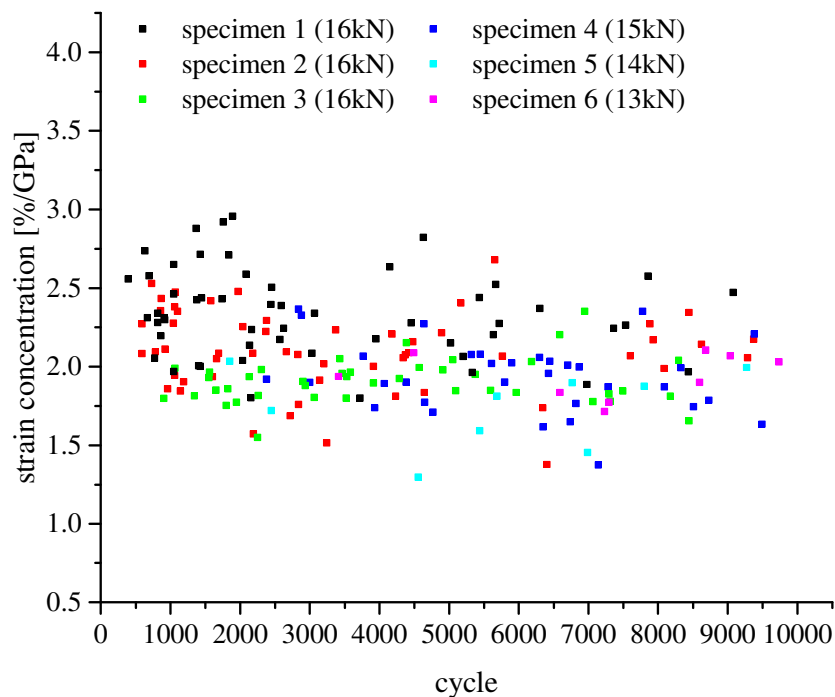
Figure 5. Local strain concentration as function of cycles for cracks in specimens 1-6.

3.2. Digital image correlation in combination with acoustic emission

Acoustic emission is a method that provides far more sensitivity for damage accumulation measurements than digital image correlation, since damage events can also be detected on the microscale. Within the scope of this work, both methods were tested and validated against each other on the basis of the detection of the inter-fibre cracks. Figure 6 shows the position of the inter-fibre cracks evaluated by digital image correlation plotted against the positions of the cracks determined by localized acoustic emission sources. For this purpose, only data from both methods was evaluated, which has mutual correspondence in a time interval of 10 seconds (= 20 cycles). The crack position evaluated from digital image correlation shows a high correlation with the localized acoustic emission sources. The linear regression results in a slope of 1.05+/-0.018 mm/mm for the graph shown in Figure 6, indicating a high degree of correlation of the two methods.
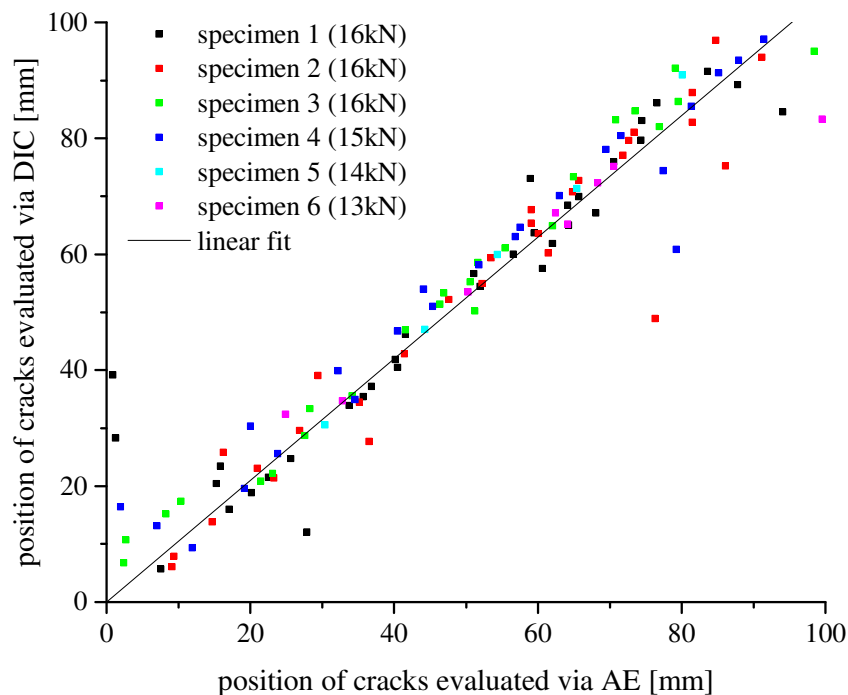
Figure 6. Position evaluated from DIC measurements as function of the position evaluated from AE measurement for all cracks that were detected in a matching time interval.

4. Conclusions

The low-cycle fatigue tests up to 10000 cycles ranging from 52% to 64% of the static tensile strength were successfully combined with digital image correlation and acoustic emission measurements. This provides valuable information about the occurrence of inter-fibre cracks in the 90° layers of the specimen with the layup configuration of $[0/90_2]_{sym}$. The method of digital image correlation offers precise measurement of the crack position to determine the crack distance and the crack density. This serves to assess to what extent the crack saturation has an influence on the further behaviour of the specimen under cyclic loading. Furthermore, the time of initiation of individual cracks could be determined with an accuracy of 5 seconds due to the triggered recording mode. It has been shown that specimens tested at higher loads (16kN) already show 50% of the cracks at 3000 of 10000 cycles, compared to specimens at lower loads, at which the inter-fibre cracks occur significantly later. Furthermore, the strain concentration provides information on the behaviour of the individual inter-fibre cracks. It was shown that the immediate vicinity of the cracks has a massive influence on the local strain values at the position of the crack. This allows evaluation of the mutual influence of neighbouring

cracks. This will act as promising input for the assessment of the influence of local strain concentrations and global strains on the contribution of fatigue failure in composite materials.

During the fatigue tests, acoustic emission signals were recorded. Previously, studies about the combination of digital image correlation and acoustic emission in static testing [1, 12] were carried out, which confirm a correspondence of the acoustic emission activity and strain concentration at the position of damage. In this work, the good correspondence in interpretation of digital image correlation and acoustic emission of single inter-fibre cracks was further confirmed. The combination of both methods therefore offers the possibility to create a comprehensive data basis for damage analysis and failure accumulation in low-cycle fatigue, since the acoustic emission analysis continues to detect damage activity on a microscale and thus allows investigating its contribution to fatigue failure. Considering that the detected inter-fibre cracks with energy higher than 0.2×10^{-4} represent only 0.5% of all localized damage events, acoustic emission measurements offer a huge potential for formation of smaller damage, which are not accessible by the digital image correlation measurements.

Acknowledgment

References

[1] M.G. Sause. *In Situ Monitoring of Fiber-Reinforced Composites.* Springer International Publishing, 2016.

[2] G.R. Irwin. Analysis of stresses and strains near the end of a crack traversing a plate. *Journal of Applied Mechanics* 24: 361–4, 1957.

[3] H. Tada, G.R. Irwin, P.C. Paris. *The stress analysis of cracks handbook.* 3rd ed. American Society of Mechanical Engineers, 2000.

[4] A.P. Vassilopoulos, T. Keller. *Fatigue of Fiber-reinforced Composites.* Springer London, 2011.

[5] B. Harris. *Fatigue in composites: Science and technology of the fatigue response of fibre-reinforced plastics.* CRC Press, 2003.

[6] S. Wicaksono, G.B. Chai. A review of advances in fatigue and life prediction of fiber-reinforced composites. *Proceedings of the IMechE* 3, 227: 179–95, 2012.

[7] A.P. Vassilopoulos. *Fatigue life prediction of composites and composite structures.* Woodhead Publishing, 2010.

[8] A.T. Zehnder, J. Carroll, K. Hazeli, R.B. Berke, G. Pataky, M. Cavalli et al. *Fracture, Fatigue, Failure and Damage Evolution,* Volume 8. Springer International Publishing, 2017.

[9] M. Bourchak, Farrow I.R. Fatigue damage assessment of UD CFRP composite laminates under spectrum loading using acoustic emission, *Jeju Island, Korea,* August 21-26, 2011.

[10] N. Schorer, M.G. Sause. Identification of failure mechanisms in CFRP laminates using 3D digital image correlation. *20th International Conference on Composite Materials*, *Copenhagen, Denmark,* July 19-24, 2015.

[11] C. Li, F. Ellyin, A. Wharmby. On matrix crack saturation in composite laminates. *Composites Part B: Engineering* 5, 34: 473–80, 2003.

[12] C. Flament, M. Salvia, B. Berthel, G. Crosland. Local strain and damage measurements on a composite with digital image correlation and acoustic emission. *7th European Workshop on Structural Health Monitoring*, *La Cité, Nantes, France,* July 8-11, 2014.